Available online at www.sciencedirect.com
SCIENCE DIRECT®
Journal of Nuclear Materials 343 (2005) 101–115
journal of nuclear materials
www.elsevier.com/locate/jnucmat

# Assessment of cavitation–erosion resistance of 316LN stainless steel in mercury as a function of surface treatment

S.J. Pawel *

*Metals and Ceramics Division, Oak Ridge National Laboratory, P.O. Box 2008, Oak Ridge, TN 37831-6156, USA*

**Abstract**

A vibratory horn apparatus was used to assess the cavitation–erosion resistance in mercury of annealed type 316LN stainless steel as a function of surface treatment. The modifications examined included cold-working, welding, laser-alloying of the surface, and two low-temperature carburization treatments. Based on general wastage (measured by weight loss) and depth of surface relief/pitting, the best cavitation–erosion resistance in Hg was achieved with one of the carburization processes for which the substrate material was oriented such that inclusion stringers were parallel to the test surface. The most successful carburization process was found to be similarly effective for both wrought and welded 316LN.


## 1. Introduction

The Spallation Neutron Source (SNS) will generate neutrons via interaction of a pulsed (60 Hz) 1.0 GeV proton beam with a liquid mercury target. The high energy pulses are expected to give rise to thermal-shock induced pressure waves in the Hg which, after reflection of the waves from containment surfaces, will result in negative pressure transients and cavitation in the target liquid [1,2]. Some of the energy released during the collapse of the cavitation bubbles near the containment surface will be manifested in a jetting action of liquid at extreme velocity that can potentially erode the containment material.

Based on a favorable combination of factors, including resistance to corrosion by Hg, well-characterized behavior in a neutron radiation environment, and absence of a significant ductile–brittle transition following irradiation, the prime candidate target containment material for the SNS [3] is type 316LN stainless steel. However, previous tests have indicated that annealed 316/316LN is susceptible to potentially significant pitting and erosion damage from cavitation in Hg using a split Hopkinson pressure bar (SHPB) apparatus [4], in-beam exposures [5,6], and a vibratory horn [7–10]. Of particular concern is the observation that pit depths resulting from relatively brief SHPB and in-beam exposures (order of 10–200 cavitation pulses/events), if linearly extrapolated over the anticipated target service life of ~500 million pulses, would prematurely threaten the integrity of the target containment.

Potentially, the cavitation–erosion resistance of annealed 316LN may be improved by hardening the material via surface treatments or cold-work. In an extension of a previous effort [10], this work utilized a vibratory horn technique to assess and compare various treatments to improve cavitation–erosion resistance of 316LN in mercury.

* Tel.: +1 865 574 5138; fax: +1 865 241 0215.
*E-mail address:* pawelsj@ornl.gov

0022-3115/$ - see front matter © 2005 Elsevier B.V. All rights reserved.
doi:10.1016/j.jnucmat.2004.10.170

## 2. Experimental

Cavitation–erosion tests were performed using a titanium vibratory horn and the general test methodology described in ASTM G-32 [11]. The test specimens had a surface area of 180 $mm^2$ exposed to cavitation and were attached to the vibratory horn tip via a threaded shank. The horn tip oscillated at a fixed frequency of 20 kHz and was set to generate a peak-to-peak vibrational amplitude of approximately 25 μm. The rapid reciprocating displacement of the specimen surface at the horn tip induces the formation and collapse of cavities in the liquid near the specimen surface, and cavitation–erosion damage can be quantified by measurement of specimen weight loss and/or penetration depth as a function of exposure time. A jacketed stainless steel container holding about one liter of high purity Hg (same Hg used for all tests) permitted temperature control for each test by circulating a water/ethylene glycol mixture from a constant temperature bath via insulated tubing. All tests reported here were performed at a mercury temperature of 25 °C; test temperature was measured with thermocouples in the Hg – one placed about 1.5 cm below the test surface and another placed near the container ID at the depth of the test specimen. The precise temperature of the test surface, if different from the local Hg temperature, is not known. Temperature control was required for all tests (even brief ones) because the Hg cavitation medium is rapidly heated by the energy input of the sonication process. In all cases, the specimen surface was immersed 25 mm below the surface of the Hg in the center of the container, which was open to room air. The crystal case of the vibratory horn was wrapped with a water-cooled copper coil to reduce over-heating of the piezoelectric crystal, which nevertheless occasionally over-heated and halted operation of the unit during a test.

Table 1
Composition of master heat of 316LN stainless steel from certified mill report

| Element | Wt% | Element | Wt% |
|---|---|---|---|
| C | 0.009 | Cr | 16.31 |
| Mn | 1.75 | Mo | 2.07 |
| P | 0.029 | Co | 0.16 |
| S | 0.002 | Cu | 0.23 |
| Si | 0.39 | N | 0.11 |
| Ni | 10.2 | Fe | Balance |

All specimens (details appear in [10]) were prepared from 316LN stainless steel with the composition given in Table 1. The baseline 316LN coupons were machined from mill-annealed stock, polished to a 600-grit finish, then re-annealed at 1020 °C for 30 min in an evacuated quartz tube. Several variations of this condition were also examined, including:

(a) mill-annealed material in the as-machined condition; this material exhibited significant surface relief (lathe rings) and disturbed metal (meaning plastically deformed material over a limited volume, increased hardness of a thin layer and additional residual stress) on the test face, and was not re-annealed after machining,

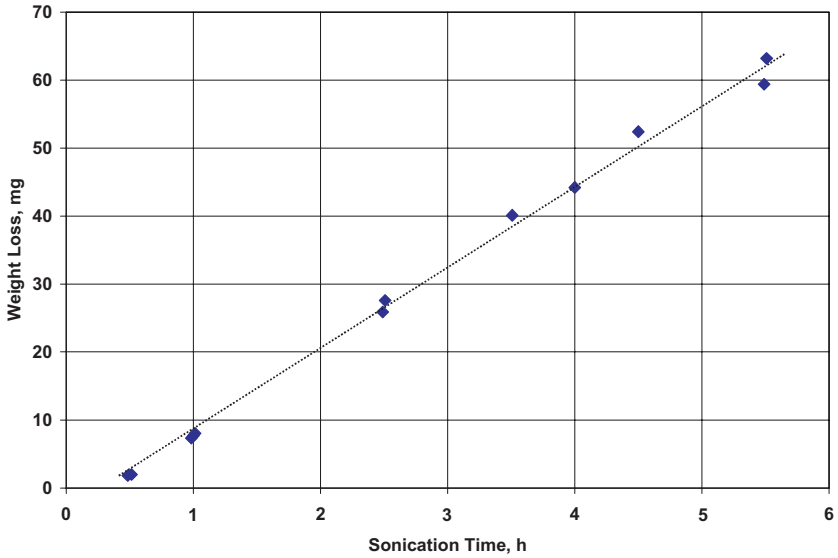


Fig. 1. Specimen weight loss as a function of exposure time in the vibratory horn for fully annealed 316LN in Hg at 25 °C. Data points here represent a total of seven different specimens.

(b) baseline material that was exposed to a proprietary surface hardening treatment termed Kolsterising® (a registered trademark of the Bodycote Company, Apeldoorn, Netherlands); in this low temperature carburization process, up to several weight percent solid-solution carbon is diffused into the stainless steel substrate to a depth of nominally about 33 μm in the standard treatment; a limited number of specimens received a 'heavy' treatment to an approximate depth of 47 μm,

(c) baseline material that was exposed to a proprietary surface hardening treatment termed low-temperature colossal super-saturation (process developed and patented by the Swagelok Company, Solon, OH; the designation LTCSS® is in the process of being registered to collaborators at Case Western Reserve University in Cleveland, OH); the initial activation treatment and carburization time/temperature/atmosphere are somewhat different for LTCSS® compared to Kolsterising® but the end result remains a supersaturated solid solution of carbon in the surface of the component so treated, to a standard depth of about 20–22 μm for the LTCSS® process,

(d) baseline material that was welded in three different ways: manual electron beam, automated electron beam, and automated tungsten-inert gas (TIG) to develop prototypic weld structures with small amounts of residual ferrite; in addition to testing the as-welded structures, specimens of each type of welding also received the 33 μm Kolsterising® treatment,

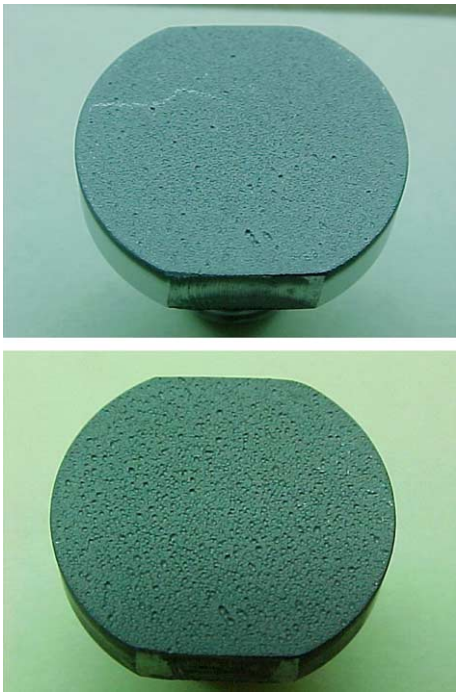

Fig. 2. Fully annealed 316LN following cavitation testing in Hg for 2.5 h (top) and 5.5 h (bottom). Both photographs are of the same specimen at different exposure times. Actual specimen diameter is about 16 mm.

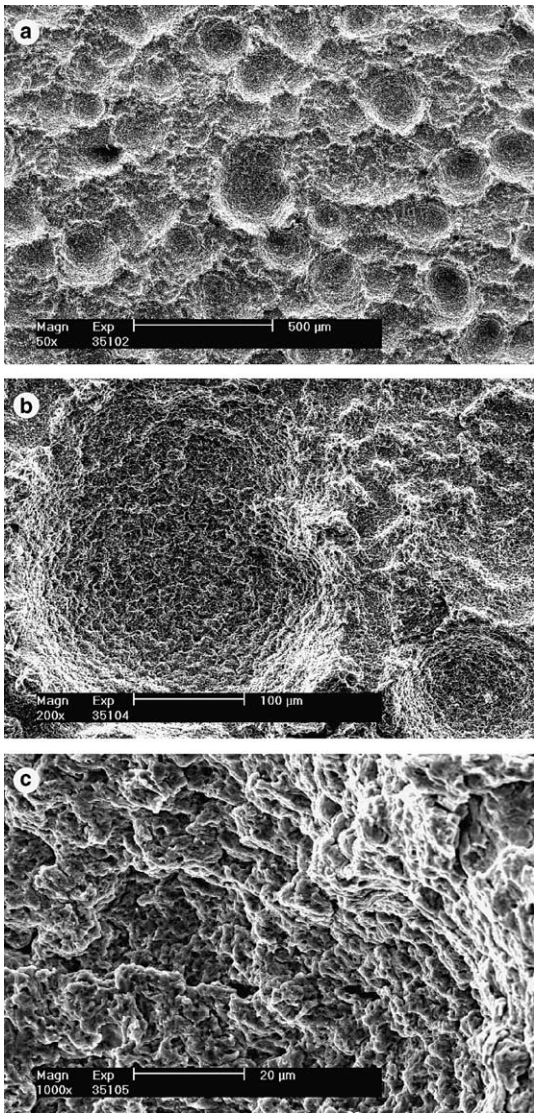


Fig. 3. SEM images of baseline 316LN specimen following 5.5 h sonication in Hg. (a) at top, pit-like surface relief on generally roughened surface; (b) middle, shows magnified view of the pit in the center of (a); (c) highest magnification, showing detail – similar to mechanical tearing – at the edge of the pit.

(e) baseline material that was laser-modified on the surface; Mn was placed on the surface of coupons and melted into the surface to create a material with a high work hardening coefficient to resist cavitation damage; two levels of composition modification were examined – 316LN with about 2% Mn or about 8% added to the surface, each to a nominal depth of 200–300 μm,
(f) mill-annealed plate that was rolled at room temperature to develop 50% cold-work in the structure; specimens were subsequently machined from the cold-worked plate and polished to a 600-grit finish.

Cavitation testing typically consisted of vibratory horn exposures of 1–2 h, oftentimes in a series to accumulate extended exposures up to 20 h in duration. At the end of each individual exposure period, coupons were allowed to sit in room air for about 10 min, during which time Hg wetted on the post-test surface invariably beaded such that slight tapping removed most of the Hg from the specimen. Subsequently, specimens were ultrasonically treated in an aqueous solution containing sulfur species to chemically bind residual Hg, followed by rinsing in water, ultrasonic cleaning in acetone, and drying with forced-air. Specimens were then weighed and, periodically, also examined microscopically for estimates of surface relief as well as average and maximum pit depths. Selected specimens were also examined with the scanning electron microscope at various exposure intervals.

## 3. Results and discussion

### 3.1. Data interpretation

There is no precise correlation between the damage rate/intensity produced at the tip of the vibratory horn and potential cavitation damage in the SNS target. Unpublished estimates of Hg cavitation pressure in the SNS target compared to the vibratory horn tests tend to indicate that the conditions imposed by the vibratory horn in this examination are not as aggressive as those anticipated in the SNS target under full-power operation. In addition, a more subtle difference between these experiments and cavitation in the SNS target is that in the latter, the target surfaces will receive pressure pulses generated at some distance while in the present vibratory horn experiments, the test surfaces themselves create pressure pulses via external vibrational motion. Nevertheless, the vibratory horn can be used to rapidly accumulate a significant number of cavitation pulses (comparable to the number in the expected service life of a target) to compare the relative performance of materials/treatments under equal conditions for the purpose of screening a variety of different surface treatments.

Evaluation of cavitation–erosion damage based on weight loss is perhaps an adequate general comparison between materials/treatments, but it assumes a uniform wastage over the specimen surface, which is not always the case [12]. Even mean depth of penetration on the specimen surface assumes a relatively uniform attack,

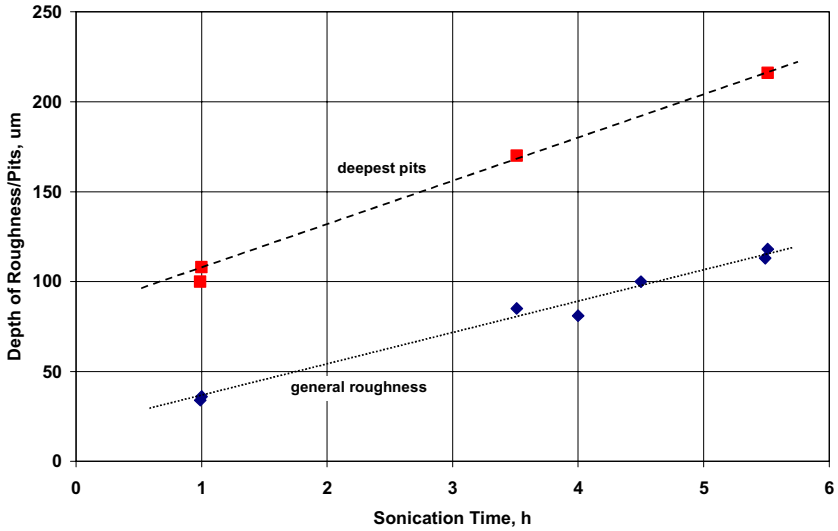


Fig. 4. Surface relief data for fully annealed 316LN specimens exposed to cavitation conditions in Hg at 25 °C as a function of exposure time. General roughness data represents the average of eight areas on each specimen, and the deepest pit data is for the single deepest pit on the specimen surface at the given exposure time.

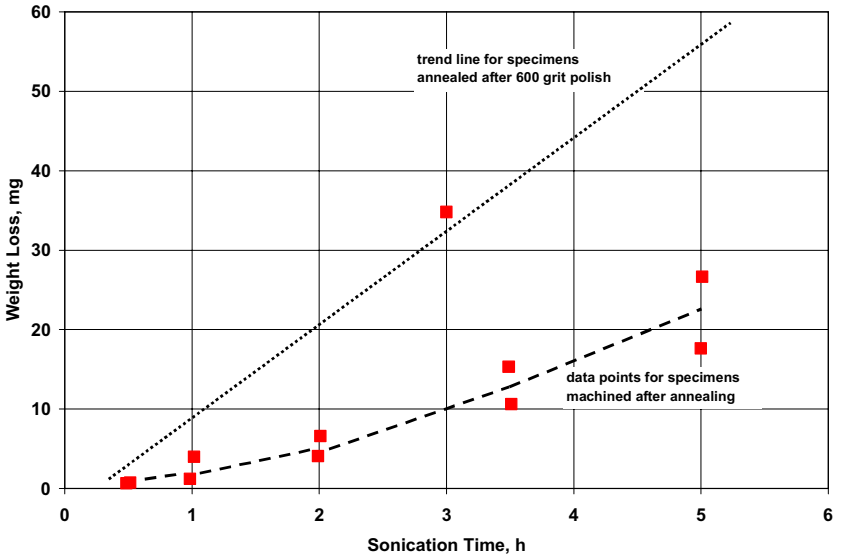


Fig. 5. Comparison of weight loss for 316LN specimens machined after annealing (data points representing five different specimens) and specimens annealed after machining and polishing (trend curve only from Fig. 1). The trend curve for the specimens machined after annealing does not consider the 'outlier' data point at 3 h sonication time.

but it is clearly the deepest penetration that is of primary concern from a target performance standpoint. In the results presented here, non-uniform wastage resembling pits is common. It is not clear whether the apparent pits form as a result of a single cavitation pulse for which specific and perhaps rare conditions (proximity of pulse to the test surface, pressure associated with the pulse, etc.) are aligned in such a way as to maximize damage to the surface, or whether the apparent pits form as a result of fluid mechanics that – for reasons unknown – focus the location of numerous pulse impacts at a limited number of sites on the test surface. Making this mechanistic distinction is beyond the scope of this investigation, which was focused on relative comparison of surface treatments to improve resistance to the apparent pitting independent of the mechanism. Because the wastage is non-uniform, both weight change and penetration data will be reported insofar as possible to support this comparison in the following sections. Other details of data interpretation may be found in Ref. [10].

### 3.2. 316LN baseline condition

Fig. 1 shows the specimen weight loss as a function of cavitation time for the fully annealed 316LN material. This graph, like many others in this document, was generated using several test specimens. A few of the specimens were exposed a relatively short duration, cleaned and weighed, and returned the horn tip multiple times to accumulate extended exposure time. Other specimens were exposed only once for a specific duration. Each data point in Fig. 1 (and in the other graphs as well) represents a specific specimen result rather than an average weight loss for many specimens at a given exposure time.

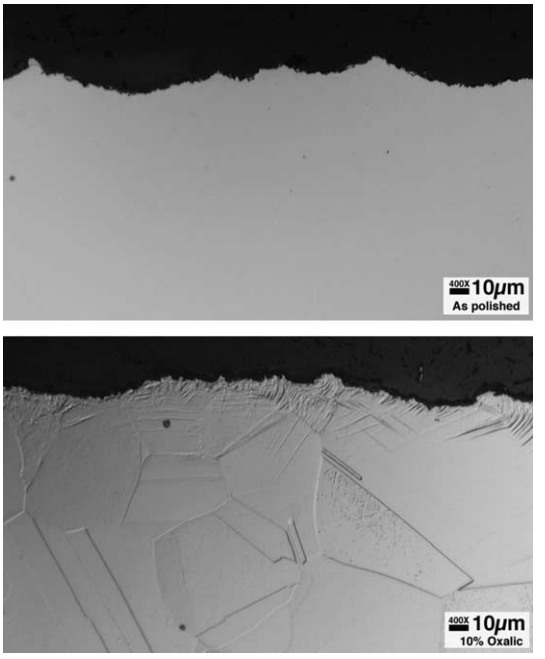


Fig. 6. Cross-section of 316LN specimen machined after annealing after exposure for 3.5 h in the cavitation test. Top: unetched, showing approximately 20 μm surface relief. Bottom: etched, showing less relief in area with residual cold-work (as indicated by slip lines near surface).

After a brief incubation time, during which it seems probable that initial micro-cracks coalesce to effect *bulk* material loss [7,12], the slope of the trend curve in Fig. 1 is approximately constant over the period shown and corresponds to about 11.8 mg/h weight change. Assuming a perfectly uniform weight loss for the specimens with maximum exposure, a thickness loss of approximately 40–45 μm might be expected (based on specimen surface area of 180 $mm^2$ and density of 7.9 $g/cm^3$) compared to the pre-test thickness. However, no average thickness change could be detected with a micrometer. It is clear from Fig. 2, however, that weight loss is not particularly uniform for the annealed material, with relatively large pits scattered over the test surface. Fig. 2 is

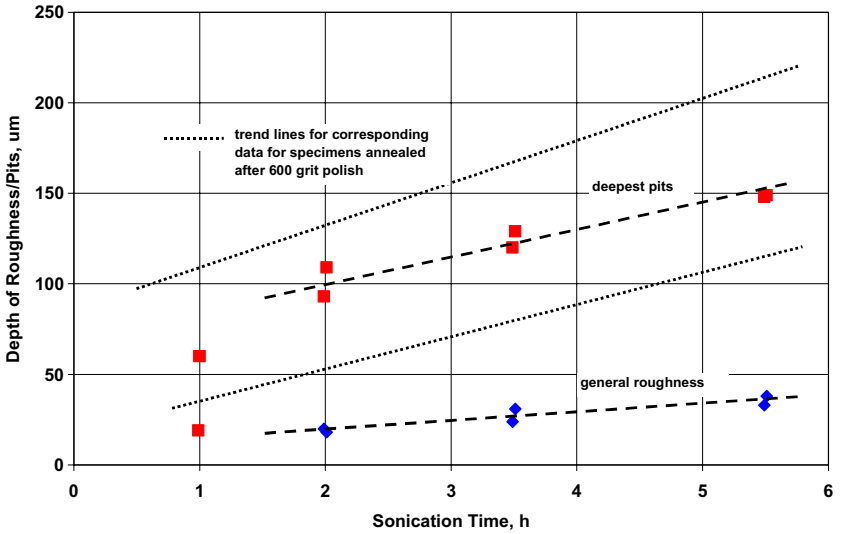


Fig. 7. Surface relief data for 316LN specimens machined after annealing compared to specimens that were annealed after surface preparation was complete.

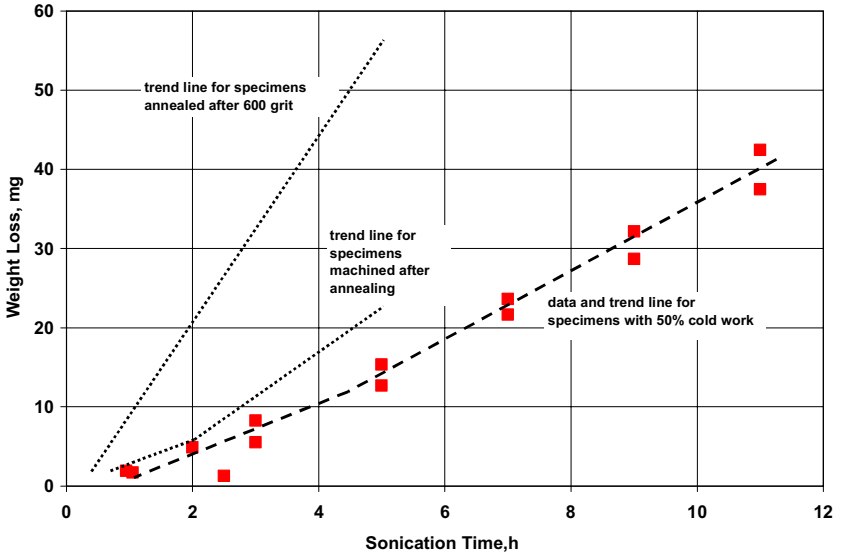


Fig. 8. Comparison of cavitation erosion resistance in Hg for 316LN with 50% cold-work (data points with trend line) with annealed material (trend lines only). Three total specimens used to generate the data points for the 50% cold-worked material.

also representative of the observation that the number of relatively large pits tends to increase with exposure time rather than individual pits becoming significantly larger. For example, the short row of pits near the bottom center of the photograph was first detected after 2.5 h exposure, but this group of pits remained more-or-less unchanged after 5.5 h exposure.

The scanning electron microscope (SEM) was used to resolve details of the sonicated surface to facilitate ready comparison of cavitation–erosion resistance for different surface treatments. Fig. 3 shows the surface of a specimen in the baseline condition following exposure for 5.5 h. The low magnification photograph (3(a)) shows a high density of pit-like cavities superimposed on the generally roughened surface. Higher magnification photographs (3(b) and 3(c)) show the surface structure in/around the largest pit shown in (3(a)). The highest magnification photograph indicates many similarities with the structure following a primarily ductile failure of austenitic stainless steel, suggesting that the cavitation process 'tears' material from the surface.

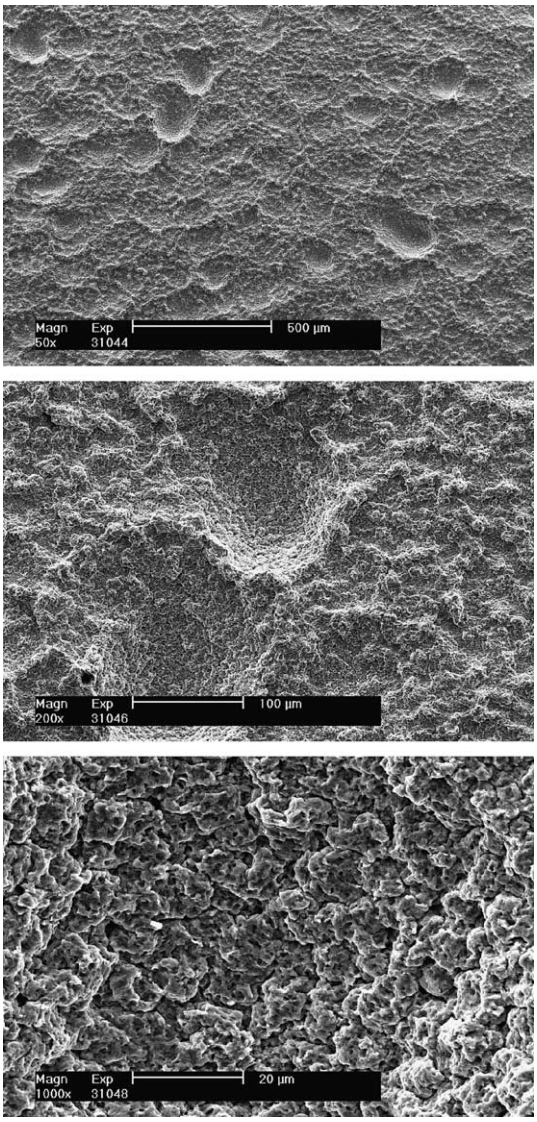


Fig. 9. SEM images of a 316LN specimen cold-worked 50% and sonicated 11 h in Hg.

The depth of surface relief/attack on the post-test specimen surface was measured using the light microscope and the calibrated fine focus knob. Each division on the knob represents a one-micron vertical movement of the microscope stage, so by sequentially focusing first on the bulk surface (relative 'high point') and then the bottom of a nearby pit, the depth of surface relief/pitting can be estimated. Fig. 4 shows data for both the nominal surface roughness as well as the deepest pits observed on fully annealed specimens of 316LN. The general roughness, which was calculated as the average relative profile height in eight fields of view on the specimen surface at 400×, changes in a roughly linear fashion with a slope of about 17 μm/h. Perfectly uniform development of surface relief to the depth indicated by the general roughness data in Fig. 4 would correspond to a weight change rate of about 24 mg/h, which is about twice the value observed in the total weight loss curve of Fig. 1. Recognize, however, that the attack is not uniform and only approximately half of any substantial area exhibits significant surface relief. Also note that the intercept of this trend line is greater than zero. Interpretation is hampered by a lack of data at very short exposure times, but the positive intercept implies that localized cavitation–erosion damage of susceptible areas occurs extremely quickly – perhaps beginning with the very first pulse. This observation is also consistent with previous results [4–6,12] indicating some pitting or surface roughness after a very few cavitation pressure cycles.

The slope of the trend curve in Fig. 4 for the deepest pits on each specimen (24 μm/h) is only slightly greater than that for the general surface roughness, while the apparent intercept is approximately four times larger. This may suggest that inclusions intersecting the test surface or other particularly susceptible inhomogeneities (exposed at the outset or that become exposed during the erosion process) are eroded quickly and completely compared to the base metal, thus accounting for the relatively sudden appearance of a limited number of rather large pits. Once the inclusion is consumed by the erosion process, the rate of further increase in local depth might be expected to conform (decrease) to the rate of change for the bulk surface. The similarity between the rate of change for the deepest pits and the general roughness in Fig. 4 suggests that this is approximately the case. It could be argued that the impact of a cavitation pressure pulse may tend to slightly harden the surface at the

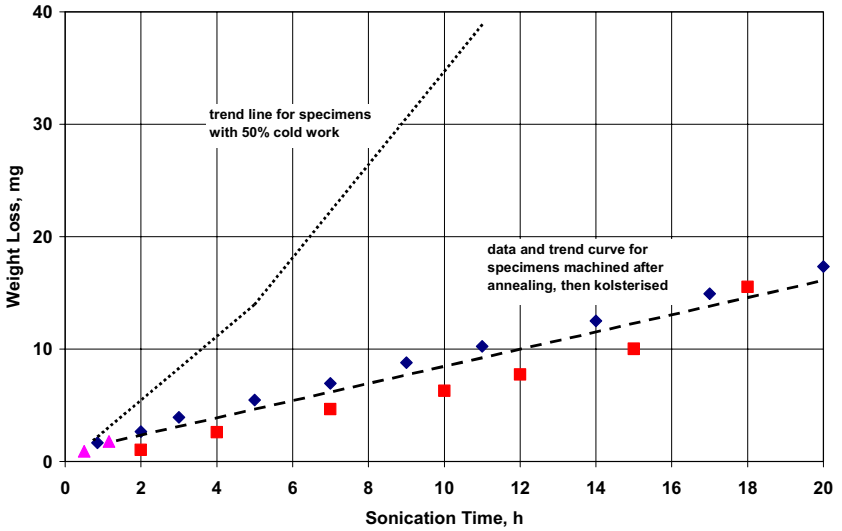


Fig. 10. Comparison of cavitation erosion resistance for 316LN with 50% cold-work with annealed 316LN receiving the Kolsterising® treatment. Three different Kolserized® specimens – represented by different data point shapes – were tested.

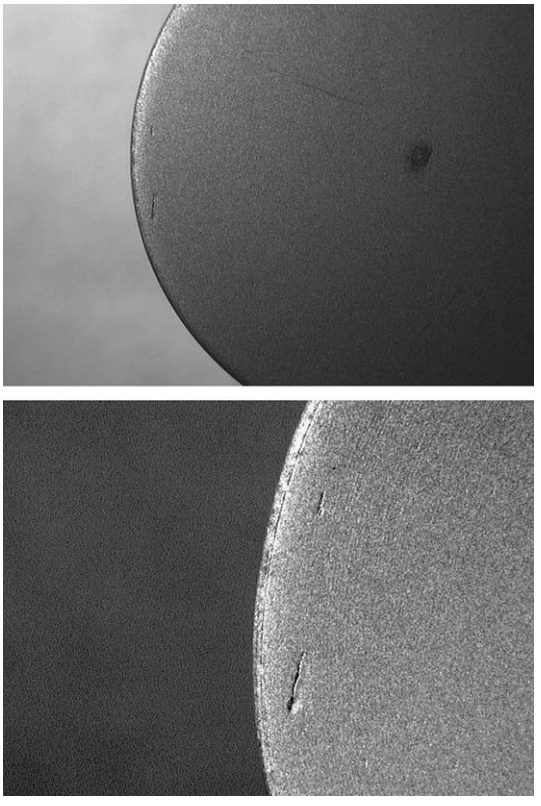

Fig. 11. Annealed 316LN specimen with the Kolsterising® treatment following 5 h of exposure. In the case shown here, the pits on the left edge of the specimen are the only ones observed on the entire specimen. The longest of the two indications is about 0.7 mm in length, and both are at least 200 μm deep.

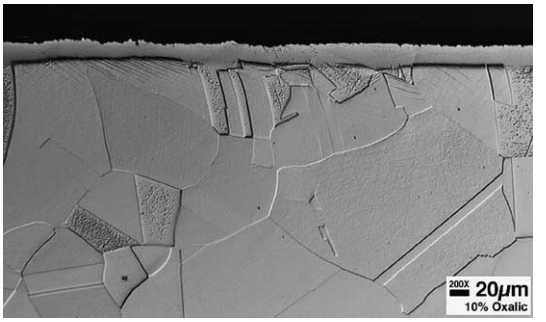


Fig. 12. Cross-section of an annealed 316LN specimen that has received the standard Kolsterisation® treatment and been sonicated for 18 h in Hg.

bottom of a pit, resulting in a slightly self-limiting nature to some of the largest pits. However, no metallographic evidence of deformation or hardening associated with the cavitation process (e.g., cross-sections through pits to show significant slip bands under/near the pit) was observed.

In contrast to localized hardening, there is the possibility that a sufficiently deep pit may actually tend to 'focus' cavitation damage pressure pulses, making previously pitted areas susceptible to a greater rate of erosion than unpitted material. Generally speaking, collapsing cavitation bubbles must be very near the containment surface – perhaps no more than 2–3 bubble diameters distant – to cause erosion damage. In principle, the focusing would result from the fact that inside a pit, a disproportionately large fraction of the Hg volume is near the pit walls, thus increasing the like-

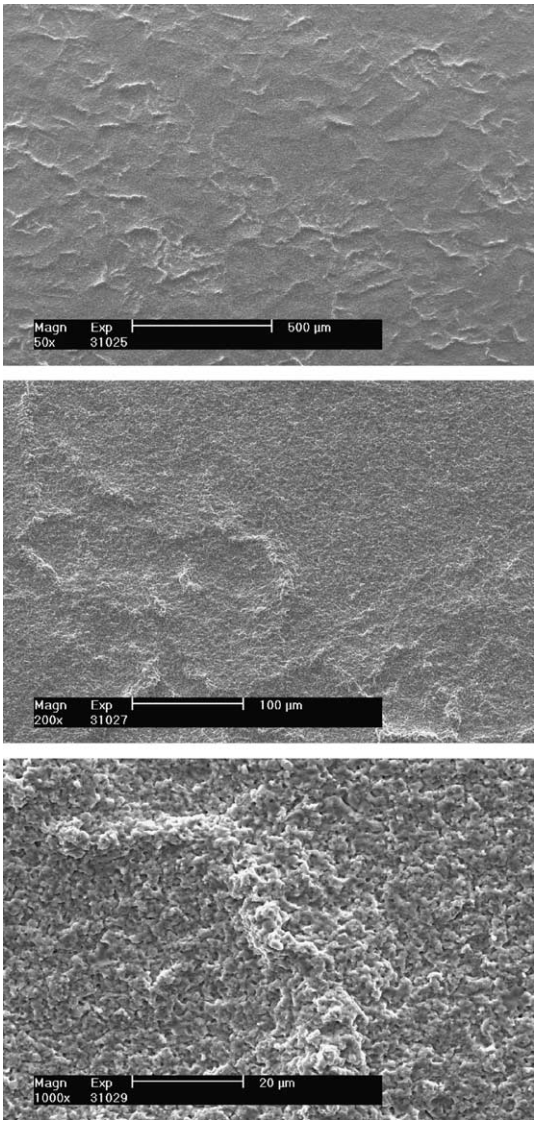


Fig. 13. SEM images of a 316LN specimen that received the standard (33 µm) Kolsterising® treatment followed by sonication in Hg for 20 h.

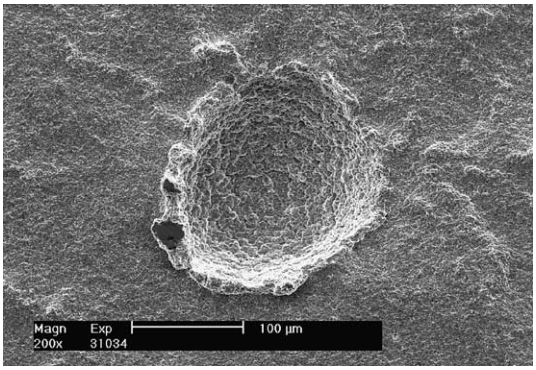


Fig. 14. SEM image of an isolated pit on a Kolsterized® surface of a 316LN specimen after sonication in Hg for 20 h.

lihood that cavitation damage, if it is occurring, would be relatively more aggressive in the pit than on a general surface. However, since the slopes of the trend curves in Fig. 4 for the deepest pit and the general roughness are so similar, this is unlikely to be a large factor for the conditions imposed by this test.

### 3.3. 316LN machined after annealing

Compared to specimens that were fully annealed after machining and polishing, specimens that were machined *after* annealing retained a slight amount of disturbed metal and surface cold-work on the test face. As the data in Fig. 5 shows, the as-machined specimen surfaces exhibited slightly improved resistance to cavitation–erosion (particularly for relatively brief exposures), due ostensibly to the slight surface hardening associated with the disturbed metal. In addition to reduced weight loss at equivalent exposure times, note that the incubation time for the specimens machined after annealing may be slightly longer than that for the baseline condition. Fig. 6 shows representative microstructures indicating the general surface roughness of 316LN specimens after sonication and near-surface slip bands from the residual cold-work of the machining process. (Additional information and photographs of as-tested surfaces for this material appear in Ref. [10].)

Note that the slope of the weight loss trend curve in Fig. 5 increases with increasing exposure for the specimens machined after annealing, suggesting that as the skin of slightly worked surface is eroded away, the specimen surfaces become more similar. In fact, one apparently 'outlier' data point (at 3 h, ~35 mg weight loss) representing material machined after annealing followed a 1-h exposure in which the weight loss was identical to another similar specimen (1 h, 4 mg weight loss). It would seem that the 'skin' of worked material was particularly thin for the specimen represented by the 'outlier' data point.

Fig. 7 shows the average depth of attack as a function of exposure time for specimens machined after annealing compared to the fully annealed material. The difference between the nominal roughness and the deepest pits is very similar for each specimen condition, but the rate of increase for nominal roughness and deepest pits is somewhat lower for the specimens machined after annealing. Also note the particularly large difference in the apparent incubation time for deep pits for the latter material; the 'skin' of cold-work appears particularly effective in delaying the onset of deep pits (or minimizing the size) during the initial stages of sonication exposure.

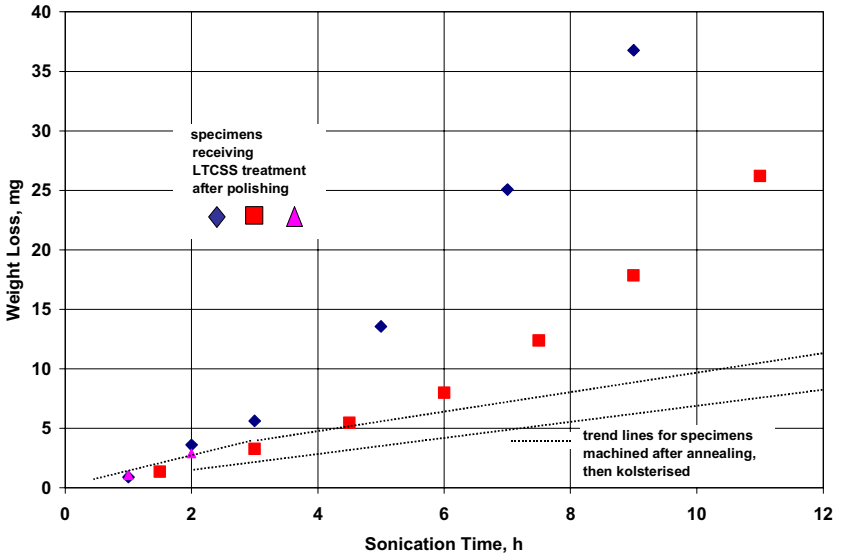


Fig. 15. Comparison of weight loss as a function of sonication time in Hg for specimens receiving the LTCSS® treatment and specimens receiving the Kolsterisation® treatment. Different symbols represent different individual specimens with the LTCSS® treatment.

### 3.4. 316LN with 50% cold-work

Fig. 8 compares cavitation weight loss data for 316LN with 50% cold-work (300–350 DPH, or $HR_C = 30–35$) with the fully annealed specimens (115–120 DPH, or $HR_B = 55–60$). The graph indicates that 50% cold-work increases cavitation resistance – measured by relative rate of weight loss – by a factor of about 3–4 depending on whether the slope for the 50% cold-worked material is determined early or late in the test.

Following sonication, the nominal surface roughness of the cold-worked specimens was minor with very few pits in number/depth compared to the annealed specimens. Fig. 9 contains SEM photographs of a 50% cold-worked specimen following 11 h sonication in Hg. Although the exposure time here is twice that for the fully annealed specimen shown in Fig. 3, it is clear that the development of surface relief on the cold-worked specimen is modest compared to that for the fully annealed specimen. (Other SEM photographs of 50% cold-worked specimens appear in Ref. [10].) For the two 50% cold-worked specimens exposed for 11 h, one exhibited an average surface roughness of 52 μm with no pits deeper than that value, and the other specimen (the one with lower total weight loss) exhibited an average surface roughness of only 38 μm, but it had a few significant pits, the deepest of which was 152 μm deep.

### 3.5. 316LN with Kolsterising® treatment

Specimens of annealed 316LN subsequently machined into test buttons were subjected to the Kolsterising® treatment prior to testing. Fig. 10 compares weight loss for the Kolsterised® specimens with that for 50% cold-worked specimens, and it is clear that, based on relative weight change rates at extended exposure times, the Kolsterised surface improves cavitation–erosion resistance by a factor of about five (slope about 4.2 mg/h for 50% cold-worked and 0.8 mg/h for Kolsterised® material).

The nominal surface roughness of the sonicated Kolsterised® specimens is very minor – on the order of 5 μm or less – even after 20 h of exposure. However, it was a routine observation that the Kolsterised® specimens

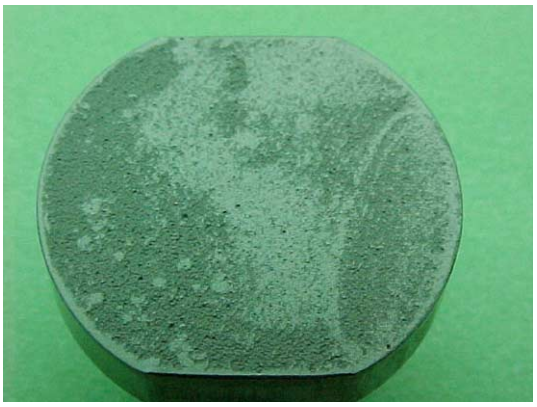

Fig. 16. Photograph of a specimen with the LTCSS® treatment after 9 h sonication. Rough (dark) areas behave similarly to annealed material with no surface treatments while smooth (light) areas are relatively resistant to cavitation–erosion.

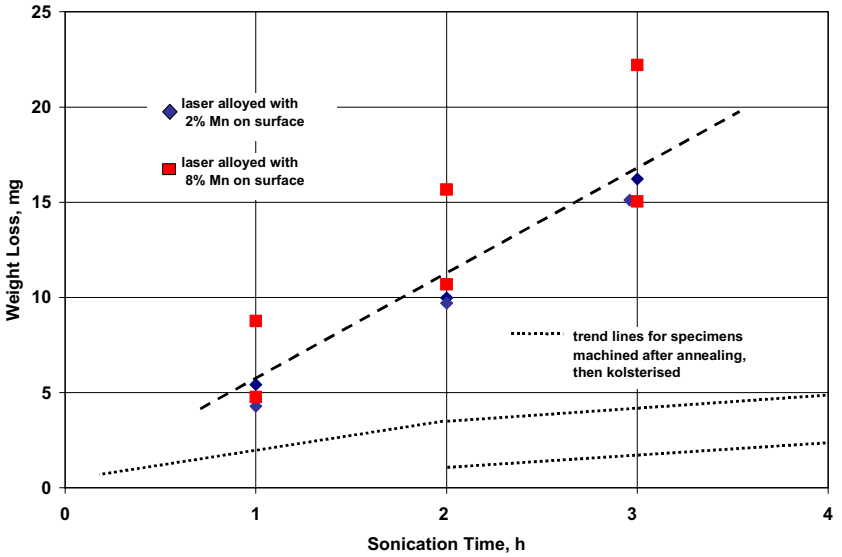


Fig. 17. Comparison of weight loss as a function of sonication time in Hg for laser-modified 316LN with Kolsterised® 316LN (base metal annealed in both cases).

exhibited a small number of deep pits (up to 5–6 per specimen in the worst cases) on an otherwise essentially smooth post-test surface. Fig. 11 contains a representative example of this observation, showing the appearance of the only two pits on the test surface following 5 h of exposure. Following 20 h exposure, the same two pits were observed (no other significant pits had developed), but the mouth of each pit had become somewhat wider and more rounded. Upon initial observation (1 h exposure), the deepest of these pits was approximately 200 μm. The depth increased to at least 300 μm during the next hour of exposure, but beyond this depth the microscope does not work well for determining depth due to physical limits of the focusing stage.

Fig. 12 is representative of the nominal surface of an annealed 316LN specimen with the Kolsterising® treatment. In this particular case, the specimen had been sonicated in Hg for 18 h and the surface layer is slightly roughened. The unexposed specimen representing this condition had an almost perfectly smooth surface with a layer thickness of about 32–35 μm compared to the thickness of 20–25 μm for the specimen exposed 18 h. This observation indicates that although the cavitation–erosion resistance of the Kolsterised® surface is relatively high, some amount of relatively uniform erosion does occur. Note that a uniform material loss of about ~10 μm corresponds to essentially the entire weight change observed for the specimen exposed 18 h, implying that the contribution to the weight loss by the limited number of large pits is relatively small. The Kolsterised® layer appears to have an expanded fcc structure based on the observation that there is continuity of austenite grain boundaries across the interface between substrate and the carburized layer (although heavy etching and high magnification are required to observe this tendency). Further, the slip lines in the substrate beneath the carburized layer indicate high localized stresses associated with the carburization process. Micro-hardness profiles of the specimen cross-section indicated the carburized layer was at least 850 DPH (~$HR_C$65) everywhere with a surface hardness value approaching 1100 DPH.

Fig. 13 contains SEM photographs (for comparison with Figs. 3 and 9) showing the relative extent of surface relief on sonicated specimens receiving the Kolsterisation® treatment. In this particular case, the exposure

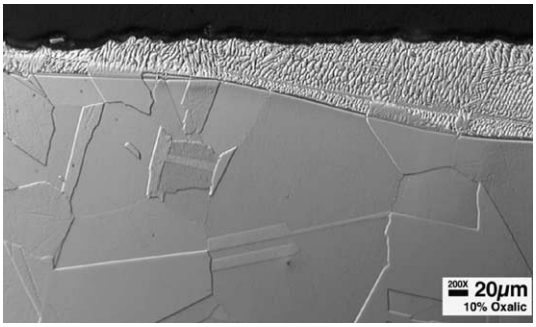


Fig. 18. Cross-section of annealed 316LN with surface modified by laser-alloy (~8% Mn). This specimen has been sonicated in Hg for 3 h. Note the large variation in remaining thickness of the modified layer.

Fig. 19. As-welded specimens of 316LN. Top: TIG weld. Bottom: automated electron beam weld. In all cases, the substrate condition was annealed 316LN with an as-machined surface.

time was 20 h (almost 4× and 2× the exposure period for the specimens represented in Figs. 3 and 9, respectively) and the general surface relief is <5 μm. Fig. 14 shows an isolated pit on the surface of this specimen; note that in the pit, the surface roughness is similar to that of untreated material, perhaps because the pit has penetrated beyond the depth of the surface treatment.

It appears that elongated inclusions perpendicular to the test surface are largely responsible for the pitting pattern observed on the Kolsterised® test specimens. The particular heat of 316LN used to fabricate these specimens is somewhat dirty in the metallurgical sense and examination of polished cross-sections revealed inclusion stringers up to about 400 μm in length. The non-austenitic inclusion material will not be hardened by the carburization process, so in locations where the inclusions intersect the surface (or lie just below it, such that minor surface roughening can expose the inclusion to the cavitation–erosion process), rather deep and angular pits can appear quite suddenly during testing. Fabricating specimens with an orientation such that the inclusions were parallel to the test surface substantially mitigated this type of pitting. Weight change as a function of exposure time was not dramatically influenced, but the number and – more importantly – depth of pits was reduced significantly.

Other variations on the surface condition of the 316LN specimens receiving the Kolsterizing® treatment were also examined under cavitation–erosion conditions in Hg. Specimens which were polished (600 grit) prior to Kolsterisation® gained 2.5× as much mass from the carburizing treatment as those in the as-machined condition (these received the 'heavy' treatment to a depth of about 47 μm), but weight loss and pitting in the cavitation tests were indistinguishable from specimens receiving the standard treatment. In addition, specimens were etched to remove inclusions exposed to the surface prior to Kolsterising®. This treatment reduced the number of deep pits observed per specimen but did not entirely eliminate them. Finally, 50% cold-worked material with inclusions oriented parallel to the test surface was also given the standard Kolsterisation® treatment. Weight loss after this treatment was indistinguishable from other Kolsterisation® treatments as a function of sonication time, but it did produce the absolute minimum of pit rate/depth among these specimens, with only one pit deeper than 25 μm observed in all cases of exposure up to 10 h (deepest was 60 μm). It is perhaps significant that the company providing the Kolsterised® specimens was not confident that the highly cold-worked structure would accept the carburization treatment. However, as measured by cavitation–erosion resistance, it is clear that the Kolsterising® of 50% cold-worked 316LN was successful.

### 3.6. 316LN with LTCSS® treatment

In an effort to include an alternate hardening treatment among the conditions examined here, specimens of annealed and polished (600 grit) 316LN were given the LTCSS® treatment. The hardness profile (maximum hardness and slope) associated with this treatment was substantially similar to those observed for the Kolsterising® process, except that the depth of treatment was much less (20–22 μm vs 30–35 μm) for the nominal LTCSS® treatment. As shown by the graph in Fig. 15, the cavitation–erosion resistance as measured by weight loss for the LTCSS® specimens was somewhat inferior to that of Kolsterised® specimens, particularly at extended sonication times. Based on examination of the post-test specimens, it appears that significant areas of the LTCSS® specimens began to respond to sonication similarly to untreated specimens, indicating that the hardening treatment was not uniform (sufficiently thin that it was penetrated in some areas). Fig. 16 is representative of this observation, showing relatively smooth areas (little attack/roughening, similar to the Kolster-

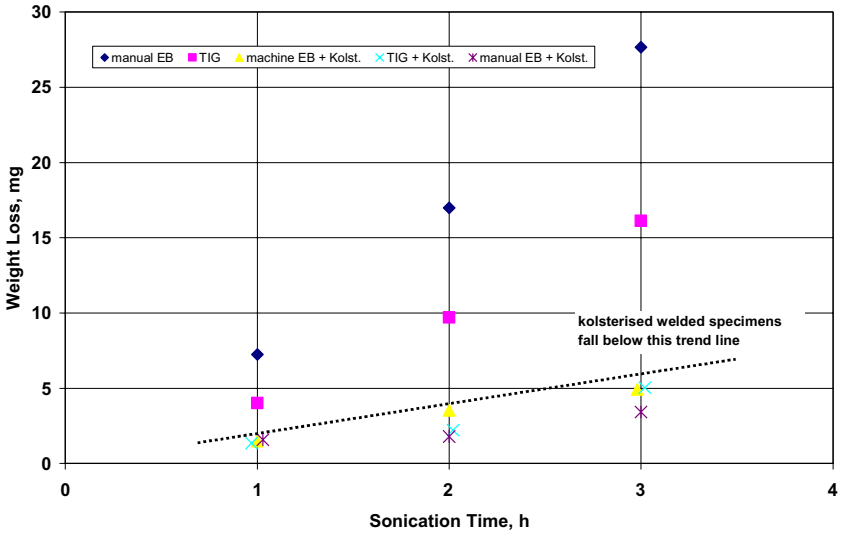


Fig. 20. Weight loss data as a function of sonication time in Hg for as-welded 316LN specimens compared to as-welded specimens receiving the standard Kolsterisation® treatment.

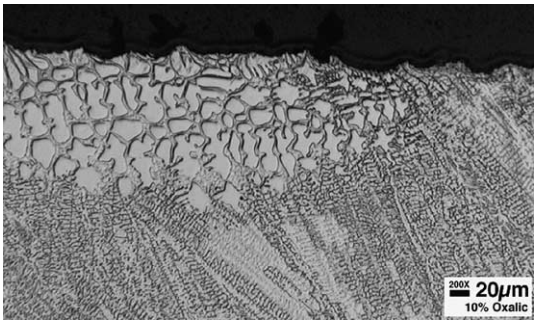


Fig. 21. Cross-section of an as-welded (TIG) cavitation button following sonication in Hg for 3 h. This location reveals only modest surface relief and shows that ferrite and austenite phases are similarly attacked.

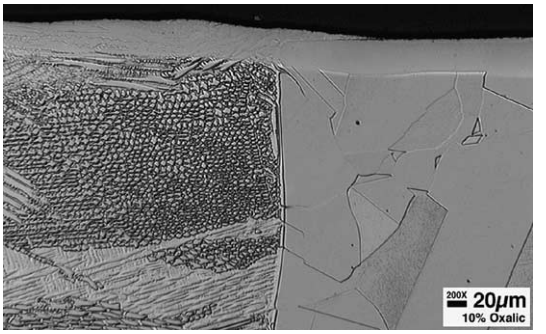


Fig. 22. Cross-section of a TIG-welded specimen following Kolsterisation® and 3 h sonication in Hg. Shows the carburization was similarly effective for both the base metal and weld area (including ferrite).

ised® specimens) as well as relatively rough/pitted areas similar to untreated specimens.

While general performance of the LTCSS® specimens may have been somewhat inferior to those receiving the Kolsterising® treatment, deep pits were not observed on the LTCSS® specimens. It is not clear if this difference is a result of a difference in the cleaning/activation steps for the respective processes or simply statistical good fortune, as the inclusions in the LTCSS® specimens were oriented perpendicular to the test face. It is the author's expectation that LTCSS® specimens treated to a depth similar to the Kolsterised® specimens would perform similarly, but this example is included here to show variable performance over the coupon surface as a function of variable carburization.

### 3.7. Surface modification by laser-alloying

Duplicate specimens modified by laser-alloying with either 2% or 8% Mn at the surface of otherwise annealed 316LN were also evaluated. In the unexposed condition, the nominal thickness of the modified composition layer was approximately 300 μm, but areas with as little as 10 μm of modified composition were observed. Compared to the Kolsterized® specimens, the laser-alloyed surface suffered a high rate of roughening and general wastage – the thickness of the alloyed layer decreased markedly with exposure time – as well as limited pitting. Specimens with 2% Mn and 8% Mn added to the surface were essentially indistinguishable in cavitation–erosion behavior measured by weight loss and extent/depth of

pitting, although one of the 8% Mn specimens (the highest weight loss in Fig. 17) had a small sliver of coating dislodged during the initial exposure period, which contributed to an abnormally high weight loss. Fig. 18 is representative of the appearance of the alloyed layer on the surface of the 316LN. In some cases, the surface of the laser-treated specimens exhibited shallow cracks following sonication in Hg.

### 3.8. Welded Specimens of 316LN

Welding processes were developed for thin plates of 316LN for which the resulting average residual ferrite was 2–3% and which could be applied to the small cavitation buttons with a minimum risk for dimensional distortion. Once suitable procedures were determined, welds were placed in the central portion of each annealed and as-machined button (residual cold-work on the working surface) using one of several successful processes. Fig. 19 shows representative examples of the as-welded test buttons.

Fig. 20 shows the cavitation–erosion weight loss data for as-welded and welded plus Kolsterised® specimens. In general, the as-welded specimens respond similarly to untreated specimens, with a weight loss (and weight loss rate) between that of the fully annealed specimens and those with residual cold-work on the surface resulting from machining. The weld areas on the as-welded specimens exhibit a nominal surface roughness about twice that of the base metal (with residual cold-work from machining) along with apparently random pitting on the order of 200 μm deep after 3 h sonication, with more modest (in depth) pitting on the base metal. For the Kolsterized® welds, however, both weight loss and pitting are very minor.

Fig. 21 shows the cross-section surface of an as-welded button containing a TIG weld following 3 h of sonication in Hg. The surface in this location reveals only modest roughening/wastage but it is representative of the observation that the ferrite phase (minor constituent) is not more readily eroded by the cavitation process than the austenite phase, which was true for all three weld types examined. Fig. 22 shows the cross-section surface of the corresponding Kolsterised® specimen at the interface between the TIG weld and the base metal following 3 h sonication. It reveals that the weld area containing ferrite and the base metal similarly accept the carburization (layer is equally thick and uniform on both substrates). This is perhaps something of a surprise, since the solubility for carbon is so much higher in the austenite phase than the ferrite phase. Fig. 22 also shows that the carburized layer resists roughening and wastage (layer essentially unchanged from the original thickness and roughness) for brief exposures (3 h in this case). Fig. 23 shows the central portion of the TIG weld shown in Fig. 22. Despite some solidification shrinkage and porosity, the carburized layer is relatively uniform and effective at limiting cavitation–erosion damage.

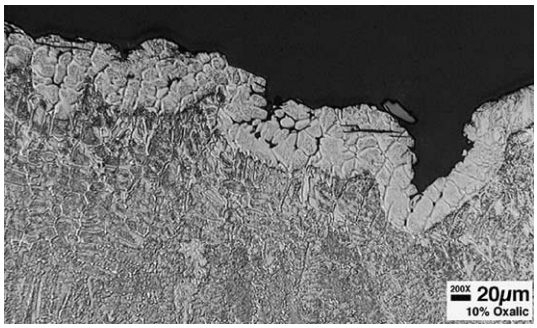


Fig. 23. Cross-section of the central portion of a TIG-welded specimen following Kolsterisation® and 3 h sonication in Hg. Despite rough/irregular surface contours with shrinkage and voids, the Kolsterisation® process appears to have effectively protected the entire surface.

## 4. Conclusions

For the conditions examined in these screening tests, the Kolsterisation® surface treatment was very effective for improving overall resistance to cavitation–erosion in Hg. General surface wastage and roughening were found to be essentially eliminated by this treatment, and obtaining favorable inclusion orientation of the substrate material with respect to the test surface mitigated isolated pitting. Further, the Kolsterisation® treatment was also effective on cold-worked and welded substrates in addition to the annealed plate. The LTCSS® treatment was somewhat less effective in extended exposures, probably due to a more shallow hardening treatment and perhaps inconsistent penetration of carbon (surface activation for this process not as uniform or effective as possible), although deep pitting was not observed on specimens so treated. Initial attempts to laser-alloy the surface layers with Mn to create a high work-hardening rate material also improved cavitation–erosion resistance compared to annealed material but much less so than for the carburization treatments.

## Acknowledgements

The author would like to acknowledge the role of many helpful individuals who supported this research effort. R.B. Ogle and F.K. Edwards Jr, provided Industrial Hygiene advice and services for controlling Hg exposures. H.F. Longmire provided metallographic services and E.T. Manneschmidt collected the SEM images in this report. D.A. Frederick and J.D. McNabb provided the welds on the test specimens. K.A. Choudhury and F.C. Stooksbury helped prepare the manuscript,

and helpful comments as well as reviews of the manuscript were provided by J.R. Di Stefano, K. Farrell, and P.F. Tortorelli. This work was funded by the Spallation Neutron Source Project.

## References

[1] R.P. Taleyarkhan, F. Moraga, C.D. West, in: Proceedings of the Second International Topical Meeting on Nuclear Applications of Accelerator Technology (AccApp98), Gatlinburg, TN, September 1998, p. 650.
[2] F. Moraga, R.P. Taleyarkhan, in: Proceedings of the Third International Topical Meeting on Nuclear Applications of Accelerator Technology (AccApp99), Long Beach, CA, November 1999, p. 301.
[3] L.K. Mansur et al., in: Proceedings of the Topical Meeting on Nuclear Applications of Accelerator Technology (AccApp 97), Albuquerque, NM, November 1997, p. 301.
[4] K. Kikuchi et al., J. Nucl. Mater. 318 (2003) 84.
[5] B.W. Riemer et al., J. Nucl. Mater. 318 (2003) 92.
[6] J.D. Hunn, B.W. Riemer, C.C. Tsai, J. Nucl. Mater. 318 (2003) 102.
[7] R. Garcia, F.G. Hammitt, R.E. Nystrom, Erosion by cavitation or impingement, ASTM STP 408, American Society for Testing and Materials, 1976, p. 239.
[8] M.D. Kass et al., Tribol. Lett. 5 (1998) 231.
[9] S.G. Young, J.R. Johnston, Erosion by cavitation or impingement, ASTM STP 408, American Society for Testing and Materials, 1967, p. 186.
[10] S.J. Pawel, E.T. Manneschmidt, J. Nucl. Mater. 318 (2003) 122.
[11] Standard test method for cavitation erosion using vibratory apparatus, ASTM G-32-98, American Society for Testing and Materials, Philadelphia, PA, 1998, p. 109.
[12] F.G. Hammitt, F.J. Heymann, Liquid-erosion failures, 8th Ed., Metals Handbook, vol. 10, American Society for Metals, 1975, p. 160.